# Analysis of the Intrinsic Uncertainties in the Laser-Driven Iron Hugoniot Experiment Based on the Measurement of Velocities *

Huan Zhang(章欢)[1,2], Xiao-Xi Duan(段晓溪)[2], Chen Zhang(张琛)[2], Hao Liu(刘浩)[2], Hui-Ge Zhang(张惠鸽)[2], Quan-Xi Xue(薛全喜)[2], Qing Ye(叶青)[2], Zhe-Bin Wang(王哲斌)[2**], Gang Jiang(蒋刚)[1**]

[1]*Institute of Atomic and Molecular Physics, Sichuan University, Chengdu 610065*
[2]*Laser Fusion Research Center, Mianyang 621900*

(Received 25 January 2016)

*One of the most challenging tasks in the laser-driven Hugoniot experiment is how to increase the reproducibility and precision of the experimental data to meet the stringent requirement in validating equation of state models. In such cases, the contribution of intrinsic uncertainty becomes important and cannot be ignored. A detailed analysis of the intrinsic uncertainty of the aluminum–iron impedance-match experiment based on the measurement of velocities is presented. The influence of mirror-reflection approximation on the shocked pressure of Fe and intrinsic uncertainties from the equation of state uncertainty of standard material are quantified. Furthermore, the comparison of intrinsic uncertainties of four different experimental approaches is presented. It is shown that, compared with other approaches including the most widely used approach which relies on the measurements of the shock velocities of Al and Fe, the approach which relies on the measurement of the particle velocity of Al and the shock velocity of Fe has the smallest intrinsic uncertainty, which would promote such work to significantly improve the diagnostics precision in such an approach.*

*PACS:* 62.50.−p, 64.30.−t DOI: 10.1088/0256-307X/33/8/086202

The equation of state (EOS) of iron (Fe) plays an important role in various fields of physics.[1−3] For example, in geophysics, the EOS and phase diagram of Fe in Mbar range is one of the fundamental issues in studying the convection process of the earth's mantle.[1−3] In recent years, several new theoretical models motivated by the difficulties in describing the pressure-induced ionization have been advanced.[3−5] To verify the reliability and accuracy of these models, it is critical to obtain precise experimental EOS data above Mbar.[3] The laser-driven Hugoniot experiment technology is one of the most widely employed techniques to obtain high-pressure EOS above Mbar, which can generate much higher pressure as high as Gbar[6,7] compared with other traditional high-pressure technologies such as gas gun,[8−10] chemical explosion[11] and Z-pinch.[12] With the great advance in laser technology and laser target physics since the 1970s, the laser-driven shock quality has been improved (e.g., the planarity of shock breakout has been optimized to be better than 0.25%[13]) which makes it possible to perform high-precision laser-driven EOS experiment platform.

Meanwhile, taking advantage of the high precision of velocity diagnostics, the impedance-match technique based on the measurement of velocities (i.e., including shock velocity and particle velocity) of the standard and the sample materials has been developed as the most widely used technique in laser-driven experiments.[14−16] The uncertainties of these kinds of experiments can be classified into two aspects according to their origins. One stems from the diagnostics, such as the uncertainty of velocities and initial density of the sample. The other kind is considered as the intrinsic uncertainty. With the improvement of diagnostics techniques, the first kind of uncertainties such as the relative uncertainty of measured shock velocity can be decreased to about 1–2%,[14] and in such a case, analyses of the intrinsic uncertainty would play an important role to obtain reliable and precise EOS experimental results.

The intrinsic uncertainty in impedance-match experiments is mainly determined by the uncertainties from the data analysis method and the EOS of the standard. The mirror-reflection approximation is a widely used data analysis method due to its simplicity, but it will deviate from the real states especially in the range of Mbar pressure and will cause large systematic uncertainties.[16,17] Another widely used method is based on a specific theoretical EOS model whose uncertainty is hard to quantify.[15,16] Celliers *et al.* developed a data analysis method,[15,16] which could not only compensate for the deviation of mirror-reflection approximation but also quantify the influence of uncertainty of the EOS of the standard.

In fact, there are four approaches based on the measurement of velocities of the standard and sample materials, which are marked as $(D_{\rm s}, D_{\rm m})$, $(D_{\rm s}, u_{\rm m})$, $(u_{\rm s}, D_{\rm m})$ and $(u_{\rm s}, u_{\rm m})$, respectively, where $D/u$ denotes the shock/particle velocity and subscript s/m

*Supported by the National Natural Science Foundation of China under Grant Nos 11305156 and 11305159.
**Corresponding authors. Email: zhebinw@vip.sina.com; gjiang@scu.edu.cn
© 2016 Chinese Physical Society and IOP Publishing Ltd

denotes the standard/unknown material. The whole intrinsic uncertainty differs depending on the experimental approach used.

In this Letter, to quantify the influence of data analysis method on uncertainty, the analysis of the mirror-reflection approximation in the Al–Fe impedance-match experiments is performed first, which shows that its deviation is too large to be ignored. Then the correction of such deviation is made with the aid of the method introduced by Celliers *et al.*,[16] the intrinsic uncertainty from the EOS of the standard in the Al–Fe experiment is studied. Finally, the intrinsic uncertainties of four different experimental approaches based on measurement of velocities are compared.

With the Rankine–Hugoniot relations, the density $\rho$, specific internal energy $E$, and pressure $P$ of the shocked material can be determined if the shock velocity $D$ or particle velocity $u$ can be measured,

$$\frac{\rho}{\rho_0} = \frac{D}{D-u}, \tag{1}$$

$$P - P_0 = \rho_0 u D, \tag{2}$$

$$E - E_0 = \frac{1}{2}(P + P_0)\left(\frac{1}{\rho_0} - \frac{1}{\rho}\right), \tag{3}$$

where subscript 0 denotes the initial state.

In the impedance match process, if we ignore the initial pressure and take the continuous boundary condition between standards and samples into consideration, the following relationships are easily deduced,

$$P_{\rm s1} = \rho_{\rm s0} u_{\rm s1} D_{\rm s1} = \rho_{\rm s0} u_{\rm s1} D(u_{\rm s1}), \tag{4}$$

$$P_{\rm m2} = \rho_{\rm m0} u_{\rm m2} D_{\rm m2}, \tag{5}$$

$$P_{\rm s2} = P_{\rm m2}, u_{\rm s2} = u_{\rm m2}, \tag{6}$$

where subscript s/m denotes the standard/unknown material, subscripts 1 and 2 denote the incident shock state in the standard and the shocked state of the sample, respectively. Noting that the relationship of $D_{\rm s1} = D(u_{\rm s1})$ is known in the standard. It is clear that the key point to solve the above equation group is how to express $P_{\rm s2}$ of the standard material correctly and conveniently.

A typical impedance-match process between Al and Fe is shown in Fig. 1, where Al will be shocked to a high-pressure state $P_{\rm s1}$ along its principal Hugoniot and Fe will be shocked to a higher pressure state $P_{\rm m2}$ along the re-shock curve of Al when the shock crosses the interface between Al and Fe.

Due to its simplicity in expression form and good approximation to the second-shocked state, the mirror-reflection approximation[16,17] becomes one of the most widely used data analysis methods, which can be expressed as

$$\begin{aligned} P_{\rm s2}(u) &= P_{\rm s1}(2u_{\rm s1} - u) \\ &= \rho_{\rm s0}(2u_{\rm s1} - u) D(2u_{\rm s1} - u). \end{aligned} \tag{7}$$

However, as the green curve shows in Fig. 1, the approximation becomes less effective as pressure goes higher. To evaluate the degradation tendency, we assume that $P_{\rm m2}$ is the real compressed state of the sample according to the EOS database by using Al SESAME[18] 3718 and Fe SESAME 2140. Then $P'_{\rm m2_}{}_D$ and $P'_{\rm m2_}{}_u$ shown in Fig. 1 are the states deduced by using the mirror reflection method with measurement of $D_{\rm m}$ or $u_{\rm m}$, respectively. The absolute and relative deviation of $P'_{\rm m2}$ from $P_{\rm m2}$ have been calculated, as shown in Fig. 2.

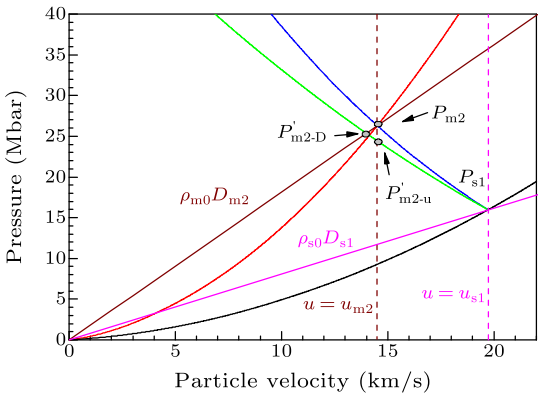


**Fig. 1.** Impedance matching construction of Al–Fe impedance-match experiment. The principal Hugoniot (black) and re-shock curve (blue) of the Al standard are from SESAME3718, Fe Hugoniot (red) from SESAME2140. Mirror reflection of the principal Hugoniot of Al is the green curve. Point $P_{\rm s1}$ denotes the incident shock state. Point $P_{\rm m2}$ is the shock state of Fe. The shock and particle velocities are represented by a straight solid line and a vertical dashed line, respectively (magenta for Al and wine for Fe). Here $P'_{\rm m2_}{}_D$ and $P'_{\rm m2_}{}_u$ denote the shock state of Fe using the mirror reflection method with measurement of $D$ and $u$, respectively.

It can be seen that $P'_{\rm m2}$ is always different from $P_{\rm m2}$ and both absolute and relative deviations become larger as pressures increase, which is in agreement with Knudson *et al.*[17] and Celliers *et al.*[16] Specifically, for the cases of $D_{\rm m}$ and $u_{\rm m}$ measurement in Al–Fe impedance-match experiments, the deviation of $P'_{\rm m2_}{}_D$ is always smaller than that of $P'_{\rm m2_}{}_u$, where the relative deviations of $P'_{\rm m2_}{}_D$ and $P'_{\rm m2_}{}_u$ around 1–40 Mbar are 0.35%–4.02% and 0.11%–8.2%, respectively.

According to the above analysis, the mirror reflection approximation could not be used directly and should be modified for the laser-driven Fe Hugoniot experiment above Mbar measurement. In 2005, Celliers *et al.* established a method for data analysis,[16] where a pressure correction factor $P_{\rm n}$ is introduced to systematically correct the mirror-reflection approximation. Then Eq. (7) becomes

$$\begin{aligned} P_{\rm s2}(u) &= P_{\rm s1}(2u_{\rm s1} - u) + P_{\rm n}(u/u_{\rm s1} - 1) \\ &= \rho_{\rm s0}(2u_{\rm s1} - u) D(2u_{\rm s1} - u) + P_{\rm n}(u/u_{\rm s1} - 1). \end{aligned} \tag{8}$$

Furthermore, such a method provides the ability to quantify the uncertainty of standard material Al for the first time. Due to completeness of uncertainty analysis, the method has been widely used in laser-driven experiments. In the following, this method will be used in the analysis of the intrinsic uncertainties in Al–Fe impedance-match experiment.

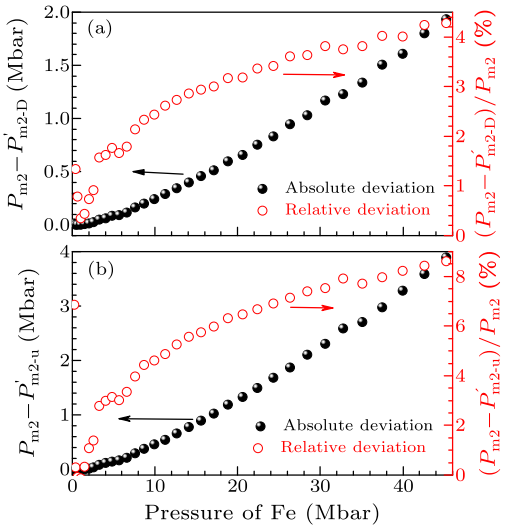


**Fig. 2.** In Al–Fe impedance-match experiments. The mirror-reflection curve of Al is used in replacement of the re-shock curve, which results in a bias in the obtained shock pressure in Fe. The absolute deviation $P_{m2} - P'_{m2}$ (left axis) and the relative deviation $(P_{m2} - P'_{m2})/P_{m2}$ (right) are shown for the measurement of the shock velocity (a) and the particle velocity (b) of Fe.

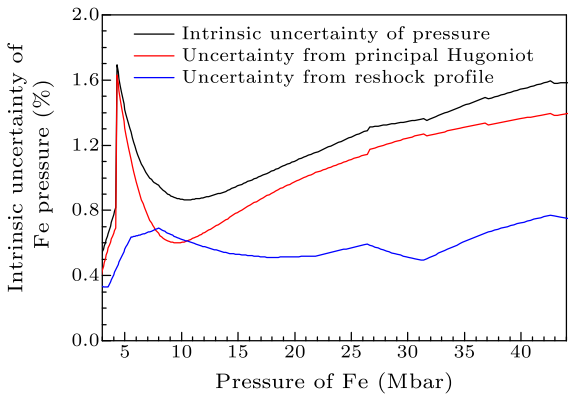


**Fig. 3.** The intrinsic uncertainty of Fe pressure from the uncertainty of Al EOS when using the $(D_s, D_m)$ approach. The uncertainties originated from the Al Hugoniot and the re-shock profile are shown by red and blue curves, respectively, and the sum is shown by solid black.

The experimental approach $(D_s, D_m)$ is the most widely used one in laser-driven experiments. The intrinsic uncertainties of this approach are calculated and the result is shown in Fig. 3. The relative uncertainty on Fe pressure from the re-shock profile is about 0.6%, smaller than about half the uncertainty from the principal Hugoniot, which indicates the latter to be the main source of the intrinsic uncertainty. The relative uncertainty from the principal Hugoniot increases with the shocked pressure due to the lack of experimental data at high pressure. There is a jump of uncertainty up to about 1.7% at 4.3 Mbar, which corresponds to the large fitting uncertainty of the principal Hugoniot of Al in the method of Celliers *et al.* In the range of 4.3–60 Mbar, the whole relative intrinsic uncertainty is about 0.88%–1.7%, which is the best accuracy achievable using $(D_s, D_m)$ approach.

The intrinsic uncertainties in impedance-match experiments based on velocity measurement would be different, depending on the experimental approach used.

A graphical illustration of the propagation of the intrinsic uncertainty is shown in Fig. 4. The incident shock state $P_{s1}$ is determined by the intersection of the principal Hugoniot with the Rayleigh line of Al or the line $u = u_{s1}$ depending on whether the shock or particle velocity of Al is measured. The uncertainty of principal Hugoniot of Al gives a set of different possible incident shock states around $P_{s1}$ from which we can calculate different possible reshock curves which will intersect with the Rayleigh line of Fe or the line $u = u_{m2}$ yielding a set of possible final states for the sample. The uncertainty of the re-shock profile gives another group of possible shock states of Fe.

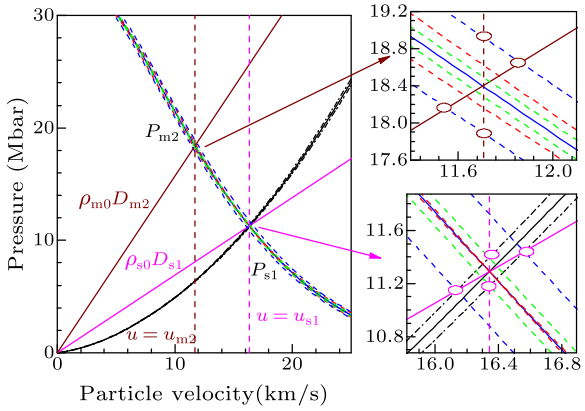


**Fig. 4.** Example of Al–Fe impedance match analysis using the method by Celliers *et al.* The solid black curve is the fitted principal Hugoniot of Al. The solid blue curve is the re-shock line. The black dashed-dotted curves are the systematic variations of the principal Hugoniot. Systematic variations of the re-shock curve obtained from the $D/u$ of Al which come from the uncertainty of principal Hugoniot are shown as blue/green curves and re-shock profile are shown as red dashed curves, respectively. Other than these differences, the states and the meaning of the curves are identical to those in Fig. 1. The lower right frame shows a detail in determining the re-shock curves from an uncertain principal Hugoniot. The upper right frame shows a detail of the shock state of Fe.

The intrinsic uncertainties of $P_{m2}$ and $\rho_{m2}$ in Fig. 4 of four different approaches are calculated and the $(u_s, D_m)$ approach gives the smallest uncertainties

with the intrinsic uncertainty of pressure about 0.64% and of density about 0.93%. The uncertainties of the $(D_s, u_m)$ approach are the largest with the intrinsic uncertainty of pressure about 2.34% and of density about 3.36%. The intrinsic uncertainties of pressure and density are 1.06% and 1.52% for $(D_s, D_m)$, and 1.48% and 2.13% for $(u_s, u_m)$, respectively.

The above difference of intrinsic uncertainty can be explained from two aspects. First, the approaches that measure the velocities of Al are compared. In the lower right frame of Fig. 4, the deviation of blue-dashed curves ($D_s$) from the re-shock curve is larger than that of the green-dashed curves ($u_s$), which indicates the priority of approaches that measure $u_s$ against those that measure $D_s$. The uncertainty of the re-shock curve obtained by using $u_s$ approaches is about 23.6% of the $D_s$ approaches.

Secondly, the approaches that measure the velocities of Fe are compared. From the upper right frame of Fig. 4, the deviation of $P_{m2}$ in the $D_m$ approaches is smaller than in the $u_m$ approaches. The deviation of $\rho_{m2}$ is more complicated and is analyzed in the following.

The shocked density of Fe can be calculated from Eq. (1) and is

$$\rho_{m2} = \frac{\rho_{m0} D_{m2}}{D_{m2} - u_{m2}}. \tag{9}$$

For the $D_m$ approaches, the density can be calculated with the particle velocity $u_{m2}$ derived by using impedance-match analysis. According to the uncertainty propagation,[19] due to the fact that the intrinsic uncertainties of $\rho_{m0}$ and $D_{m2}$ are zero, the intrinsic uncertainty of density is correlated with the intrinsic uncertainty of $u_{m2}$,

$$\left(\frac{\delta\rho_{m2}}{\rho_{m2}}\right)^2_{\rm int} = \left(\frac{u_{m2}}{D_{m2} - u_{m2}}\right)^2 \left(\frac{\delta u_{m2}}{u_{m2}}\right)^2_{\rm int}. \tag{10}$$

Meanwhile for the $u_m$ approaches, the shock velocity $D_{m2} = P_{m2}/\rho_{m0}u_{m2}$ and the density

$$\rho_{m2} = \frac{\rho_{m0} P_{m2}}{P_{m2} - \rho_{m0} u^2_{m2}}. \tag{11}$$

The intrinsic uncertainty of density is

$$\left(\frac{\delta\rho_{m2}}{\rho_{m2}}\right)^2_{\rm int} = \left(\frac{u_{m2}}{D_{m2} - u_{m2}}\right)^2 \left(\frac{\delta P_{m2}}{P_{m2}}\right)^2_{\rm int}. \tag{12}$$

In the upper right frame of Fig. 4, the relative intrinsic uncertainty of $u_{m2}$ from the $D_m$ approaches is 1.32%, which is smaller than that of $P_{m2}$ from the $u_m$ approaches, which is 2.95%, and this indicates that a smaller intrinsic uncertainty of $\rho_{m2}$ using the $D_m$ approaches than using the $u_m$ approaches.

The above analysis indicates that the $D_m$ approaches are prior to the $u_m$ approaches with smaller uncertainties for determination of both $P_{m2}$ and $\rho_{m2}$. From the above analysis, it can be inferred that the most preferred approach is the one that measures $u_s$ and $D_m$ while the combination of measurements of $D_s$ and $u_m$ will generate the largest intrinsic uncertainty.

The quantitative analysis of the intrinsic uncertainty of $P_{m2}$ and $\rho_{m2}$ of four experimental approaches are shown in Fig. 5. It can be seen that the $(u_s, D_m)$ approach has the highest precision whose relative intrinsic uncertainty is about 0.5% for $P_{m2}$ and about 1% for $\rho_{m2}$, while $(D_s, u_m)$ is the least reliable one whose relative intrinsic uncertainty is over 2% for $P_{m2}$ and 3% for $\rho_{m2}$ above 15 Mbar. The approaches of $(D_s, D_m)$ and $(u_s, u_m)$ are the second and third, respectively. The result is in accordance with the above analysis. The quantitative analysis of the intrinsic uncertainty would become much more valuable in laser-driven Hugoniot experiment whose relative uncertainty is required to be within several percent to discriminate and validate various Fe EOS theoretical models. As shown in Fig. 5, approach $(u_s, D_m)$ seems to be the best choice due to its smallest uncertainty. However, the applicability of this approach is limited significantly due to the fact that the uncertainty of diagnostics in laser-driven Hugoniot experiment to measure the particle velocity $u$ such as x-ray radiography[20,21] is much larger than the typical uncertainty for the measurement of $D$, which can be controlled to 1–2%. Considering that the intrinsic uncertainty of the $(D_s, D_m)$ approach is only about 0.5% larger than that of $(u_s, D_m)$, the $(D_s, D_m)$ approach turns out to be more reliable than the other three approaches in laser-driven Hugoniot experiment due to the fact that its diagnostics is the most precise and reliable up to now.

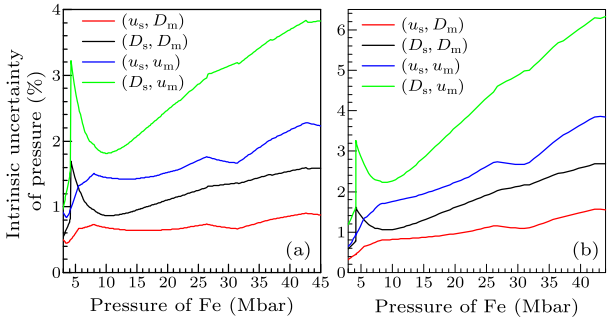


**Fig. 5.** The intrinsic uncertainties of pressure (a) and density (b) from the four different approaches. The jumps for $(D_s, D_m)$ (green curve) and $(D_s, D_m)$ (blue curve) at about 4.3 Mbar come from the uncertainty of the fitted Hugoniot of the standard material using the method of Celliers *et al.*

In summary, a detailed analysis of the intrinsic uncertainties in the laser-driven iron Hugoniot experiment is presented. There are two sources of uncertainties which are the data analysis method and

the EOS of the standard material, and the propagation of uncertainty will be influenced by the experimental approach chosen which will generate different intrinsic uncertainties. The influence of the mirror-reflection approximation and the EOS uncertainty of the standard material on the uncertainty of experimental data are quantitatively deduced for Al–Fe impedance-match experiment. Four different approaches are compared, in which different combinations of velocities are measured. The analysis shows that the intrinsic uncertainty of $(u_{\rm s}, D_{\rm m})$ approach is the smallest. However, limited by the diagnostics presently available, the $(D_{\rm s}, D_{\rm m})$ approach turns out to be more reliable and practical in laser-driven Hugoniot experiment due to its comparatively low uncertainty in diagnostics. The advantage of the $(u_{\rm s}, D_{\rm m})$ approach with the smallest intrinsic uncertainty implies that the $(u_{\rm s}, D_{\rm m})$ approach may become a better choice in the future and may stimulate the development of related diagnostics technology. The analysis method used in the present work can also be applied to other materials.

# References


[1] Benuzzi-Mounaix A et al 2002 *Phys. Plasmas* **9** 2466
[2] Andrault D et al 2012 *Nature* **487** 354
[3] Wang C et al 2014 *Phys. Rev.* E **89** 023101
[4] Piron R and Blenski T 2011 *Phys. Rev.* E **83** 026403
[5] Laio A, Bernard S and Chiarotti 2000 *Science* **287** 1027
[6] Remington B A, Rudd R E and Wark J S 2015 *Phys. Plasmas* **22** 090501
[7] Nora R et al 2015 *Phys. Rev. Lett.* **114** 045001
[8] Nellis W J et al 1981 *J. Chem. Phys.* **75** 3055
[9] Jiang G P, Huan S, Hao H et al 2013 *Acta Phys. Sin.* **62** 016201 (in Chinese)
[10] Hao B B, Feng L P, Li P et al 2013 *Chin. Phys.* B **22** 108301
[11] Boriskov G V et al 2005 *Phys. Rev.* B **71** 092104
[12] Knudson M D and Desjarlais M P 2009 *Phys. Rev. Lett.* **103** 225501
[13] Rothman S D et al 2002 *Phys. Plasmas* **9** 1721
[14] Hicks D G et al 2005 *Phys. Plasmas* **12** 082702
[15] Hicks D G et al 2009 *Phys. Rev.* B **79** 014112
[16] Celliers P M et al 2005 *J. Appl. Phys.* **98** 113529
[17] Knudson M D, Asay J R and Deeney C 2005 *J. Appl. Phys.* **97** 073514
[18] Lyon S P and Johnson J D 1992 *LANL Technical Report* No. LA-CP-98-100
[19] Bevington P R 1969 *Data Reduction and Error Analysis for the Physical Sciences* (New York: McGraw-Hill) p 96
[20] Da Silva L B et al 1997 *Phys. Rev. Lett.* **78** 483
[21] Collins G W et al 1998 *Science* **281** 1178